Report No. DOT/FAA/RD-81/85
DOT/FAA/CT-81/63

FAA WJH Technical Center
00090840

TEST AND EVALUATION OF THE AIRPORT RADAR WIND SHEAR DETECTION SYSTEM

Domenick L. Offi
William Lewis
Tai Lee
Alfred DeLaMarche

FEDERAL AVIATION ADMINISTRATION TECHNICAL CENTER
Atlantic City Airport, N.J. 08405

FINAL REPORT

FEBRUARY 1982

Document is available to the U.S. public through
the National Technical Information Service,
Springfield, Virginia 22161.

Prepared for

U. S. DEPARTMENT OF TRANSPORTATION
FEDERAL AVIATION ADMINISTRATION
Systems Research & Development Service
Washington, D. C. 20590

NOTICE

This document is disseminated under the sponsorship of the Department of Transportation in the interest of information exchange. The United States Government assumes no liability for the contents or use thereof.

The United States Government does not endorse products or manufacturers. Trade or manufacturer's names appear herein solely because they are considered essential to the object of this report.

Technical Report Documentation Page

1. Report No.	2. Government Accession No.	3. Recipient's Catalog No.
DOT/FAA/RD-81/85		

4. Title and Subtitle	5. Report Date
TEST AND EVALUATION OF THE AIRPORT RADAR WIND SHEAR DETECTION SYSTEM	February 1982
	6. Performing Organization Code: ACT-100
7. Author(s) Dominick L. Offi, William Lewis, Tai Lee, and Alfred DeLaMarche	8. Performing Organization Report No.: DOT/FAA/CT-81/63
9. Performing Organization Name and Address: Federal Aviation Administration, Technical Center, Atlantic City Airport, New Jersey 08405	10. Work Unit No. (TRAIS)
	11. Contract or Grant No.: 022-242-830
12. Sponsoring Agency Name and Address: U.S. Department of Transportation, Federal Aviation Administration, Systems Research and Development Service, Washington, D.C. 20590	13. Type of Report and Period Covered: Final Report, March 1978 - May 1981
	14. Sponsoring Agency Code: ARD-231

15. Supplementary Notes

16. Abstract

A wind shear detection system, developed by the Wave Propogation Laboratory (WPL) to operate with the Federal Aviation Administration (FAA) Airport Surveillance Radar ASR-(8), was installed and tested at the FAA Technical Center. Initial tests consisted of hardware and software shakedown and feasibility determinations. Second phase tests compared radar with aircraft and tower winds, evaluated the wind shear measurement capability under various weather conditions, and investigated the effectiveness of a simple two-azimuth pointing strategy. Final efforts consisted of observations in all-weather regimes and tests of a modified velocity-azimuth display (VAD) and a glide slope scan.

Results showed the system to be compatible with and to operate satisfactorily with the ASR-8. The processing and spectral display of clear air and precipitation returns is feasible. The accuracy of agreement between radar-measured winds and components of the aircraft-measured winds in both radially oriented flights and runway offset flights using a two-azimuth pointing technique, a glide slope scan, and a modified VAD was examined. Radar versus tower wind agreement was also examined. Potentially dangerous wind shears associated with weather during these tests were detectable. Certain system limitations were also defined and considered.

17. Key Words	18. Distribution Statement
Wind Shear Doppler Radar	Document is available to the U.S. public through the National Technical Information Service, Springfield, Virginia 22161

19. Security Classif. (of this report)	20. Security Classif. (of this page)	21. No. of Pages	22. Price
Unclassified	Unclassified	37	

Form DOT F 1700.7 (8-72) Reproduction of completed page authorized

METRIC CONVERSION FACTORS

Approximate Conversions to Metric Measures

Symbol	When You Know	Multiply by	To Find	Symbol
		LENGTH		
in	inches	*2.5	centimeters	cm
ft	feet	30	centimeters	cm
yd	yards	0.9	meters	m
mi	miles	1.6	kilometers	km
		AREA		
in^2	square inches	6.5	square centimeters	cm^2
ft^2	square feet	0.09	square meters	m^2
yd^2	square yards	0.8	square meters	m^2
mi^2	square miles	2.6	square kilometers	km^2
	acres	0.4	hectares	ha
		MASS (weight)		
oz	ounces	28	grams	g
lb	pounds	0.45	kilograms	kg
	short tons (2000 lb)	0.9	tonnes	t
		VOLUME		
tsp	teaspoons	5	milliliters	ml
Tbsp	tablespoons	15	milliliters	ml
fl oz	fluid ounces	30	milliliters	ml
c	cups	0.24	liters	l
pt	pints	0.47	liters	l
qt	quarts	0.95	liters	l
gal	gallons	3.8	liters	l
ft^3	cubic feet	0.03	cubic meters	m^3
yd^3	cubic yards	0.76	cubic meters	m^3
		TEMPERATURE (exact)		
°F	Fahrenheit temperature	5/9 (after subtracting 32)	Celsius temperature	°C

*1 in = 2.54 (exactly). For other exact conversions and more detailed tables, see NBS Misc. Publ. 286, Units of Weights and Measures, Price $2.25, SD Catalog No. C13.10:286.

Approximate Conversions from Metric Measures

Symbol	When You Know	Multiply by	To Find	Symbol
		LENGTH		
mm	millimeters	0.04	inches	in
cm	centimeters	0.4	inches	in
m	meters	3.3	feet	ft
m	meters	1.1	yards	yd
km	kilometers	0.6	miles	mi
		AREA		
cm^2	square centimeters	0.16	square inches	in^2
m^2	square meters	1.2	square yards	yd^2
km^2	square kilometers	0.4	square miles	mi^2
ha	hectares (10,000 m^2)	2.5	acres	
		MASS (weight)		
g	grams	0.035	ounces	oz
kg	kilograms	2.2	pounds	lb
t	tonnes (1000 kg)	1.1	short tons	
		VOLUME		
ml	milliliters	0.03	fluid ounces	fl oz
l	liters	2.1	pints	pt
l	liters	1.06	quarts	qt
l	liters	0.26	gallons	gal
m^3	cubic meters	35	cubic feet	ft^3
m^3	cubic meters	1.3	cubic yards	yd^3
		TEMPERATURE (exact)		
°C	Celsius temperature	9/5 (then add 32)	Fahrenheit temperature	°F

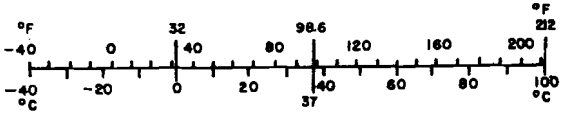

TABLE OF CONTENTS

	Page
INTRODUCTION	1
Purpose	1
Background	1
System Description	1
PHASE 1	2
Discussion	2
Summary of Phase 1 Results	10
Phase 1 Critical Conclusions	10
PHASE 2	10
Discussion	10
Summary of Phase 2 Results	16
Phase 2 Critical Conclusions	17
PHASE 3	17
Discussion	17
Summary of Phase 3 Results	26
Phase 3 Critical Conclusions	27
OVERALL SUMMARY OF RESULTS	27
CONCLUSIONS	28
RECOMMENDATIONS	29
REFERENCES	29
APPENDIX	

LIST OF ILLUSTRATIONS

Figure		Page
1	Radar Wind Shear Detection System	2
2	ASR Air Traffic Control and Wind Shear Antennas	3
3	Wind Shear Test Bed Equipment Layout	4
4	Radar Returns from Clear Air Layer and from Precipitation	6
5	Radar Wind Shear Flights, Horizontal Profile	7
6	Radar Wind Shear Flights, Vertical Profile	7
7	Radar/Aircraft Comparison: Outbound, Clear Air, Northwest Winds	9
8	Radar/Aircraft Comparison: Inbound, Clear Air, Northwest Winds	9
9	Precipitation Spectra	11
10	Clear Air Spectra	12
11	Runway 13-31, Radar Location and Data Azimuths for Wind Determination	13
12	Doppler Spectra of Heavy Rain	18
13	Clear Air Spectra on a Cold, Dry Day	19
14	Spectra of Wind and Anomalous Signals	20
15	Ground Clutter Contamination at Low Elevation Angles	22
16	Thunderstorm Gust Front Winds	24
17	Thunderstorm Wind Outflow	24
18	Contours of Constant Radial Velocity for a Typical Glide Slope Scan	25

LIST OF TABLES

Table		Page
1	Radar/Aircraft Comparison, Outbound, Clear Air, Northwest Winds	8
2	Radar/Aircraft Comparison, Inbound, Clear Air, Northwest Winds	8
3	Comparison of Radar and Aircraft Wind Components for Simulated Approaches	14
4	Presentation of the Data in Table 3 Grouped by Altitude	14
5	Comparison of Radar and Aircraft Headwind/Tailwind Components for Actual Approaches	15
6	Comparison of Radar and Aircraft Crosswind Components for Actual Approaches	15
7	Radar/Tower Average Winds and Direction/Speed Differences	16
8	System Parmeters for Glide Slope Scan	25
9	Radar/Aircraft Wind Comparisons for Simplified VAD	26

INTRODUCTION

PURPOSE.

The purpose of this project was to determine the feasibility of using pulse Doppler radar in conjunction with a new supplementary antenna and Fast Fourier Transform (FFT) data processing for the detection of hazardous low-level wind shear conditions in the optically clear atmosphere as well as in precipitation.

BACKGROUND.

Analyses of aircraft accidents have indicated that low-level wind shear has been the cause of nine terminal area accidents since 1972. Wind shear (abrupt change in wind direction and/or speed) increases or decreases the effective airflow over an aircraft's wings causing it to go above or below its intended flightpath. This is especially dangerous during critical landing and takeoff maneuvers which leave little margin for corrective action.

Significant wind shear, the dimensions of which can be tens-of-miles in width, up to 200 miles in length, and hundreds of feet in vertical extent, occurs rather infrequently (in the order of 100 to 200 hours per year at the major air terminals). The meteorological mechanisms responsible for wind shear include the thunderstorm downdraft and gust front, frontal zones, and low-level jet streams. These hazardous phenomena can occur year-round and, in the case of thunderstorm downdrafts and gust fronts, may be detected only after the fact by ground instrumentation or through pilot reports.

Under the sponsorship of the FAA Systems Research and Development Service (SRDS), Wind Shear and Wake Vortex Section, ARD-414, various solutions to the problem are being investigated. One possible solution being pursued by the Radar Section, ARD-231, is the use of specially instrumented terminal radars. In support of this effort the Wave Propagation Laboratory (WPL) of the National Oceanic and Atmospheric Administration (NOAA), under Task VII of Interagency Agreement DOT-FA76-WAI-622, conducted appropriate analyses and design efforts for the system.

Preliminary and second phase tests have been completed and previously reported (see references 1 and 2). This report summarizes those results and describes the final phase of the test and evaluation. All tests were accomplished by the FAA Technical Center, Systems Test and Evaluation Division, ACT-100H.

SYSTEM DESCRIPTION.

The system configuration is illustrated in figure 1. The Airport Surveillance Radar (ASR)-8 is one channel of the standard dual-channel radar installed in the Center's Terminal Facility for Automated System Testing (TFAST). The parabolic 15-foot diameter antenna (used for wind shear detection) was installed on the roof of the building adjoining the radar and interconnected through a waveguide switching arrangement, which allowed the radar to operate with either its standard search antenna or the wind shear antenna. The unmodified second channel was operated in an air traffic control (ATC) mode at all times. The remainder of the equipment,

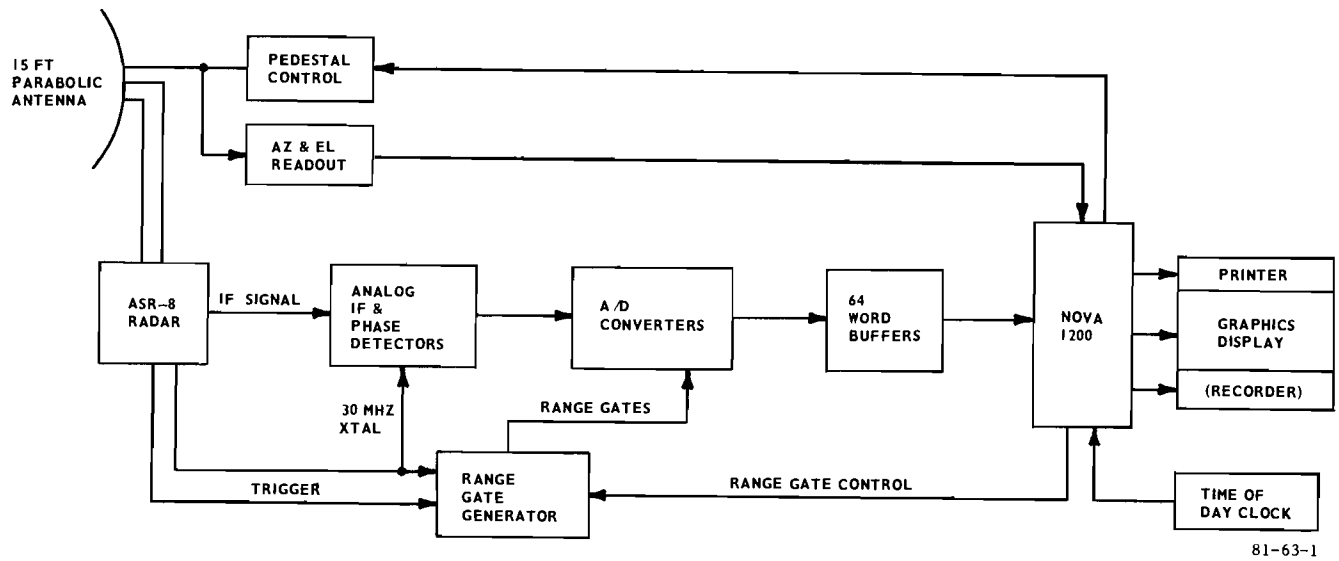

FIGURE 1. RADAR WIND SHEAR DETECTION SYSTEM

interconnected as shown in figure 1, is part of the WPL-developed system. Figures 2 and 3 are photographs of the antennas and equipment. Installation of the wind shear system did not require any modification of the ASR-8 other than rearrangement of the antenna transmission lines.

Referring to figure 1, the inphase and quadrature (I&Q) phase detector outputs are digitized. The resulting 10-bit words are stored in two 64-word buffers which are transferred to the computer as 16-bit digital I&Q video. A 128-point FFT program is used to extract the Doppler information from the radar signals. The program outputs one range gate at the selected location, acquires data, calculates the power spectrum, repeats data acquisition and calculation, averages spectra, outputs spectra to display, then steps to the next range location. After calculating and displaying spectra for each range location, the sequence is repeated and new data replaces old data on the display. In addition, the data may be recorded on the diskette-type recorder for later playback and off-line processing. Additional programs include diagnostics for troubleshooting and testing and for data reduction and analysis routines.

PHASE I

DISCUSSION.

First phase tests were performed during the period March to December 1978, with the parabolic antenna mounted on a temporary, fixed pedestal. This configuration allowed very limited position adjustment capability. Efforts included hardware and software checkout, feasibility demonstration, detection and measurement of winds in both clear air and weather, system calibration, and flight tests. Complete details are in reference 1. A brief description and summary of results are included herein.

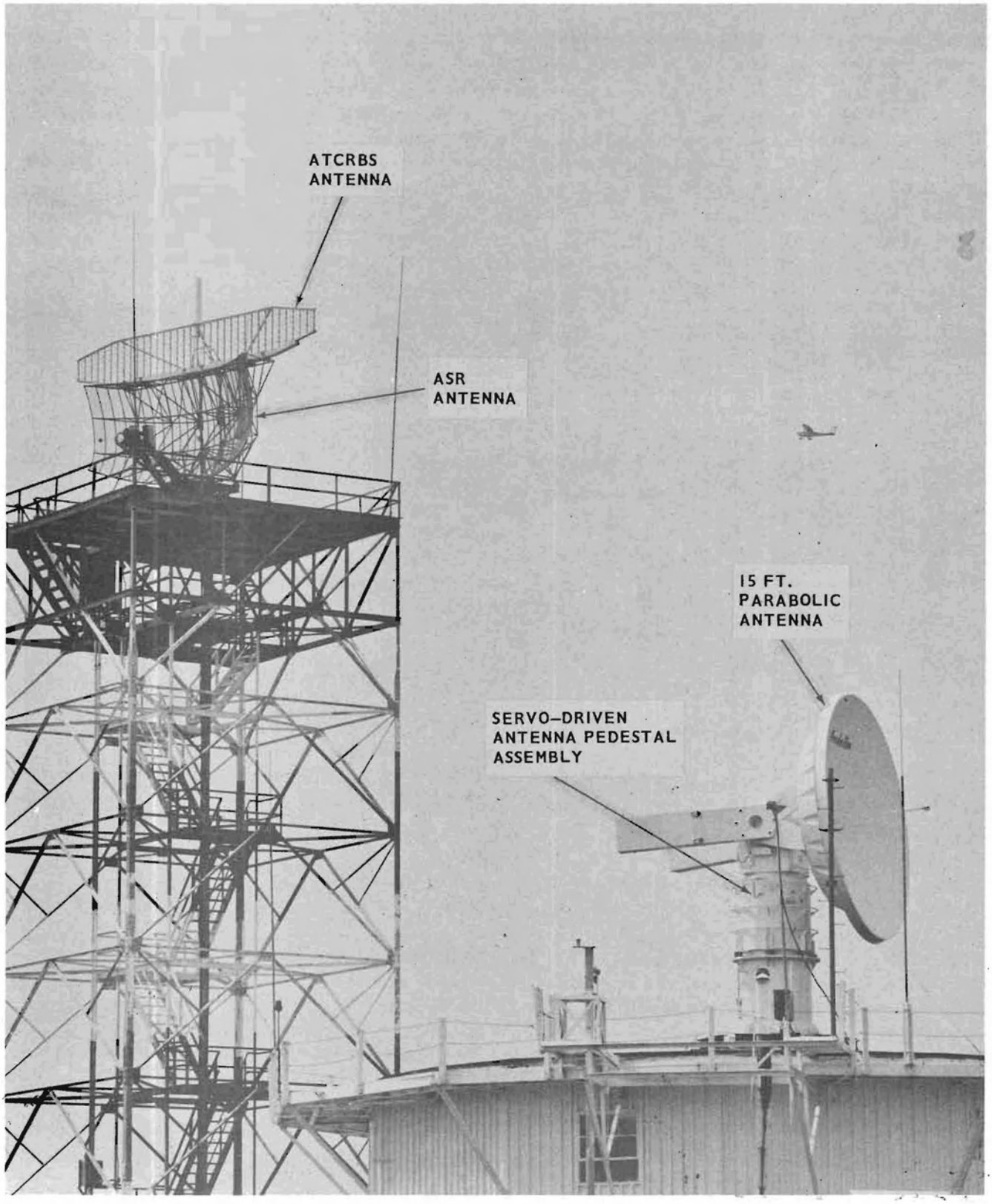

FIGURE 2. ASR AIR TRAFFIC CONTROL AND WIND SHEAR ANTENNAS

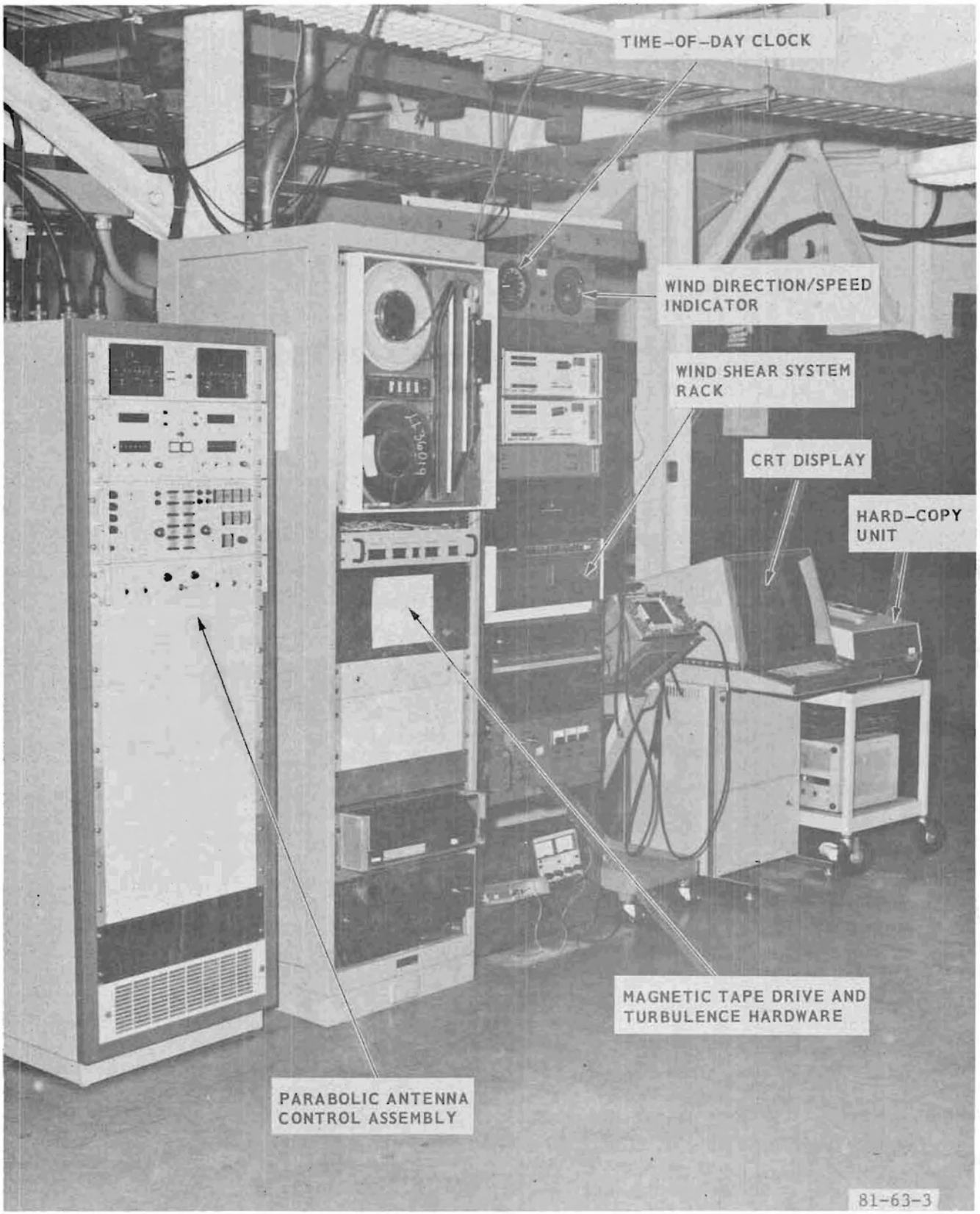

FIGURE 3. WIND SHEAR TEST BED EQUIPMENT LAYOUT

HARDWARE AND SOFTWARE EVALUATION. Except for an antenna problem (later corrected prior to start of second phase tests) all equipment operated satisfactorily.

FEASIBILITY DEMONSTRATION. The processing and spectral display of clear air and precipitation returns with the test bed system was demonstrated to be feasible.

WIND DETECTION AND MEASUREMENT. Radar returns from clear air were detectable regularly, depending on wind velocity during the period of these tests (performed in the spring and summer months when refractive index variations are generally stronger). Sensitive microwave radars can detect the scatter from these irregularities in the atmosphere and, when equipped with Doppler processing, can measure the average radial velocity and the spread of velocities.

Radar returns from rain were detectable at all times and, because of the greatly increased signal levels compared to those from clear air, demonstrated the need for automatic thresholding.

Figure 4 shows two samples of photographic data, with returns from both clear air and precipitation displayed in spectral format on the cathode-ray tube display used during these preliminary tests. Parameters of the system and display are described as follows:

DLAY - Range delay to start of measurement in microseconds (μs)
SPAC - Spacing between displayed range gates, also in μs
NORG - Number of range gates selectable from 1 to 8
NAVG - Number of Doppler spectra averaged
NSMP - Number of data points (radar pulses) used in each FFT
SCLE - Full-scale amplitude in decibels (dB)
BASE - Baseline threshold in dB

The radial wind velocity (in the pointing direction of the radar) can be estimated in each case by determining the mean of each Doppler spectrum as a function of slant range. The clear air wind was moving 25 to 30 knots negative (toward the radar) and the rain was moving at 15 to 20 knots positive (away from the radar).

Calibration. A test target generator (TTG) was used to calibrate the wind system data display in nautical miles per hour or knots. The TTG is designed to provide realistic simulated radar targets at the operating radiofrequency of the ASR-8 radar. The TTG incoming and outgoing velocity feature, along with a continuous wave (CW) signal for calibration, was used to establish the velocity calibration in 10-knot steps over a +50-knot interval.

Flight Tests. Flight tests were performed to obtain measured horizontal wind data for comparison against simultaneously recorded radar data. The aircraft used during these tests was leased, along with pilot and crew, from the University of Wyoming. A brief description of the aircraft and its instrumentation are included in the appendix. The flight tests were performed along a path which paralleled, but did not cross, the radar antenna beam, fixed in azimuth and elevation during the entire series of runs. The +3° elevation angle simulated a typical glide slope. Figures 5 and 6 show the horizontal and vertical profiles on the flightpaths.

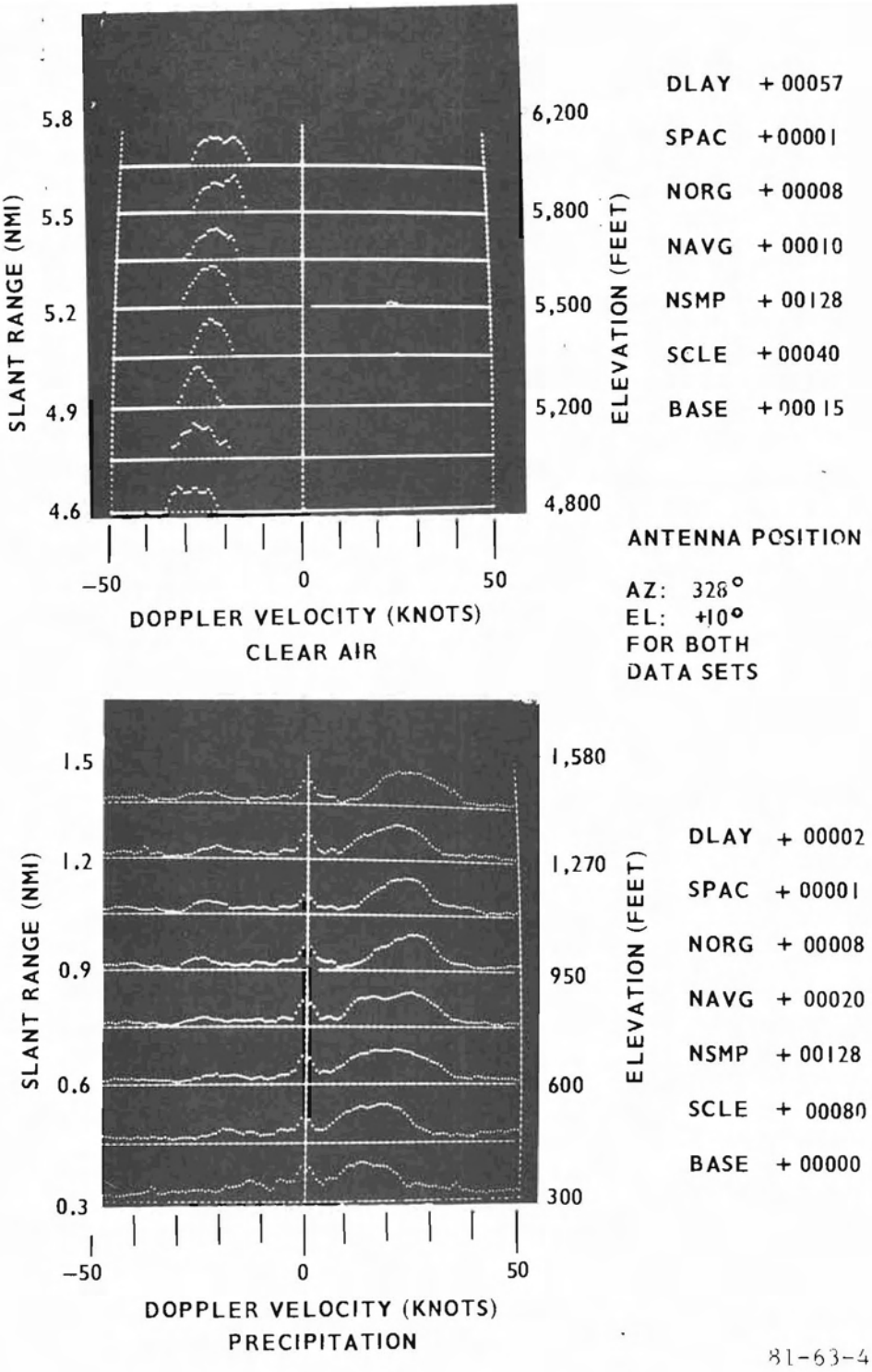

FIGURE 4. RADAR RETURNS FROM CLEAR AIR LAYER AND FROM PRECIPITATION

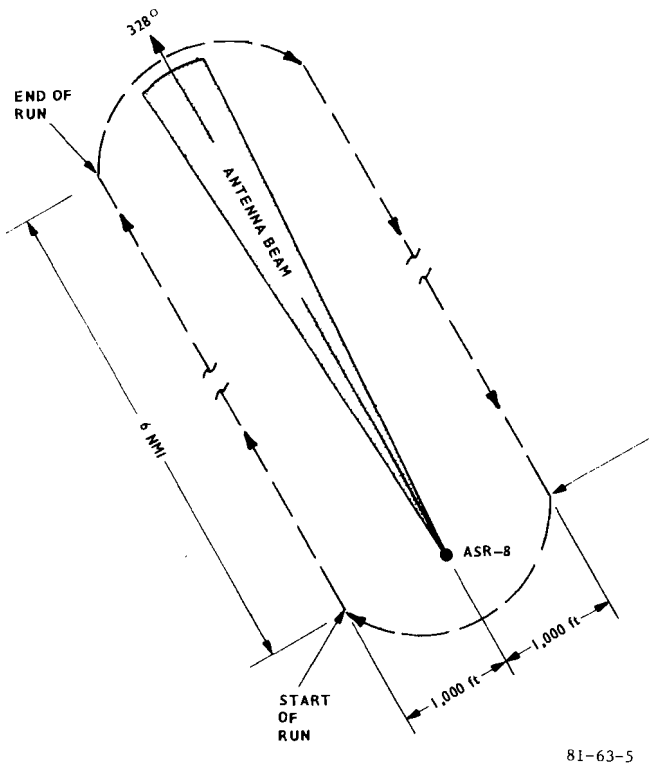

FIGURE 5. RADAR WIND SHEAR FLIGHTS, HORIZONTAL PROFILE

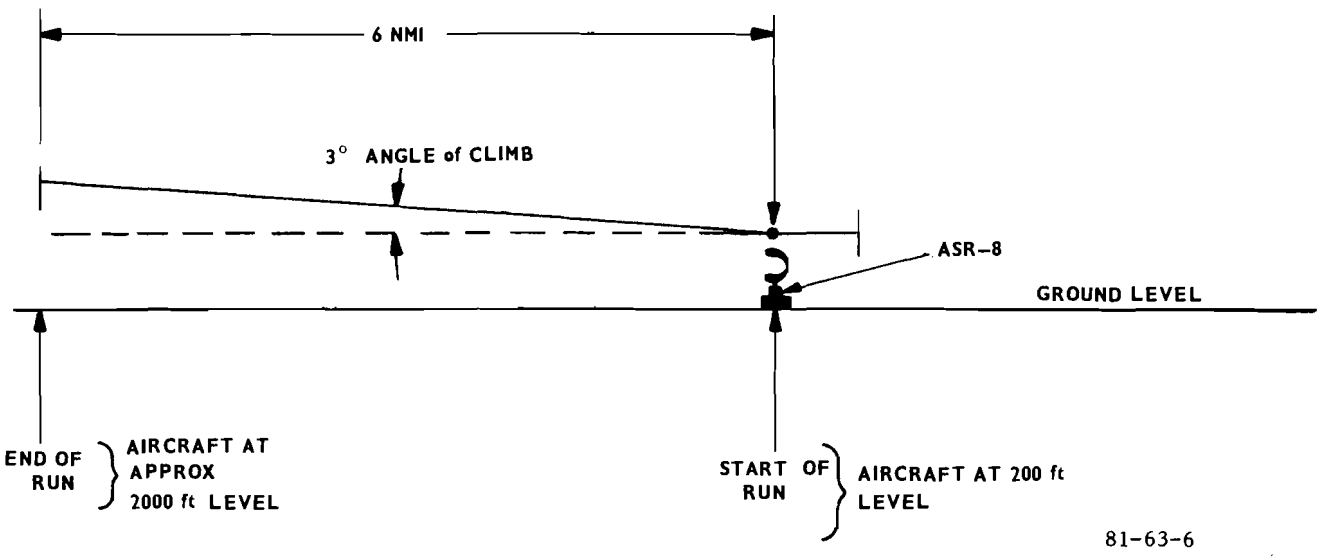

FIGURE 6. RADAR WIND SHEAR FLIGHTS, VERTICAL PROFILE

The flight tests produced ground-based and airborne data packages from a total of 25 outbound runs and 17 inbound runs over a period of 4 days. Tables 1 and 2 and corresponding graphs in figures 7 and 8 show the results for 2 of these days grouped together by meteorological regime.

TABLE 1. RADAR/AIRCRAFT COMPARISON: OUTBOUND, CLEAR AIR, NORTHWEST WINDS

Height (ft)	Radar*	A/C*	Difference*	Sigma*	Total
400	-15.7	-11.2	-4.5	3.58	9
600	-15.6	-14.8	-0.8	2.88	9
800	-15.8	-16.5	0.7	2.38	8
1,000	-14.3	-16.5	2.1	3.46	9
1,200	-15.4	-16.1	0.7	3.86	9
1,400	-16.8	-15.9	-0.8	3.78	9
1,600	-17.1	-16.2	-1.0	1.87	8
ALL	-15.8	-15.3	-0.5	3.77	61

*Components in knots (negative from 328° positive from 148°). Sigma is standard deviation of differences.

TABLE 2. RADAR/AIRCRAFT COMPARISONS: INBOUND, CLEAR AIR, NORTHWEST WINDS

Height (ft)	Radar*	A/C*	Difference*	Sigma*	Total
800	-16.0	-18.3	2.3	3.40	11
1,000	-16.8	-19.7	2.9	3.80	11
1,200	-16.1	-19.8	3.7	3.06	11
ALL	-16.3	-19.3	3.0	3.48	33

*Components in knots (negative from 328° positive from 148°). Sigma is standard deviation of differences.

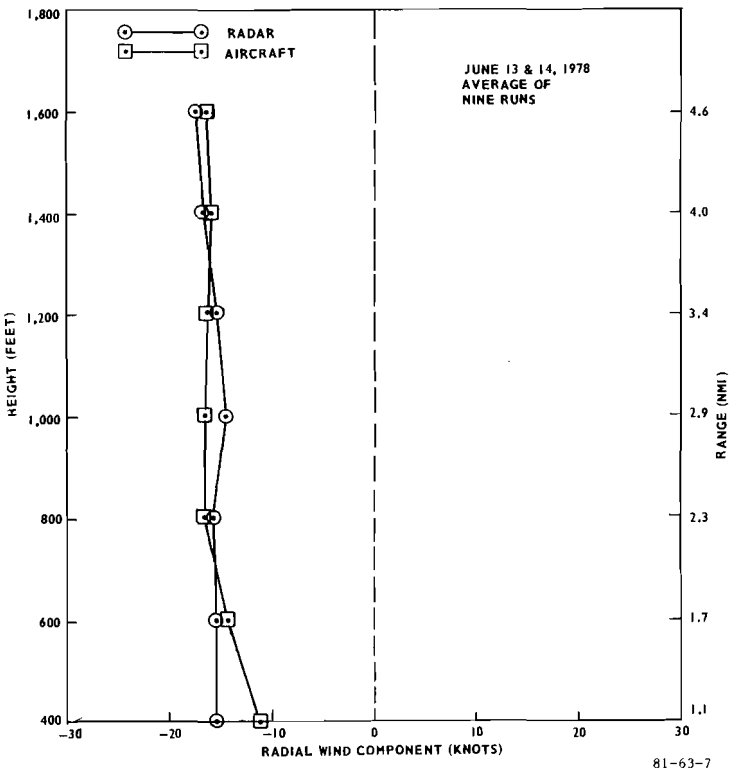

FIGURE 7. RADAR/AIRCRAFT COMPARISON: OUTBOUND, CLEAR AIR, NORTHWEST WINDS

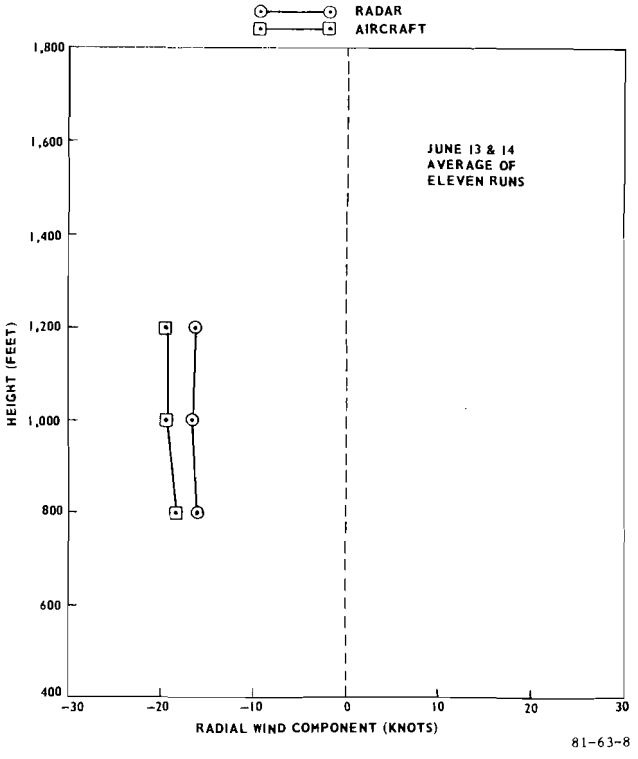

FIGURE 8. RADAR/AIRCRAFT COMPARISON: INBOUND, CLEAR AIR, NORTHWEST WINDS

SUMMARY OF PHASE 1 RESULTS.

1. Installation and integration of the system with the Technical Center's terminal radar testbed was accomplished without difficulty.

2. Operational parameters and system characteristics were determined and established.

3. A number of hardware problems were indentified and corrective action taken or initiated.

4. Returns from optically clear air as well as from precipitation were obtainable at all times when data were taken.

5. Velocity calibration of the display was completed.

6. Flight tests showed generally good agreement between simultaneously recorded radar and aircraft wind data.

PHASE 1 CRITICAL CONCLUSIONS.

The results of the Phase 1 tests showed that it is feasible to utilize a pulse Doppler radar that is designed for acquisition, processing, and spectral display of clear air and precipitation returns to measure radial wind components (headwinds and tailwinds) in the antenna pointing direction.

PHASE 2

DISCUSSION.

The second phase of the project covers the period April to December 1979 after the installation of a new antenna drive pedestal assembly. The pedestal allowed positioning of the antenna from a remote control panel and from signals provided by the computer.

A new display was also obtained which included a peripheral hard-copy unit that facilitated data reduction and analysis. Figures 9 and 10 are examples of spectral data from both precipitation and clear air returns. Wind velocity, spectral width, intensity, scaling, and threshold level information are shown in the left portion of the display. The approximate range and elevation of each measurement sample are also shown. The remainder of this section concerns further radar/aircraft wind comparisons, radar/tower wind comparisons, and the results of measuring winds and terminal-area wind shears under various weather conditions at the Technical Center. Also included is the effectiveness of antenna pointing strategies in determining the wind along the glide slope, assuming horizontally uniform wind conditions, and in the definition of system limitations and capabilities.

RADAR/AIRCRAFT WIND COMPARISON. Radar wind data were compared with aircraft wind data obtained with an inertial navigation system (INS)-equipped Technical Center Gulfstream aircraft. Two operating procedures, simulated and actual, were used.

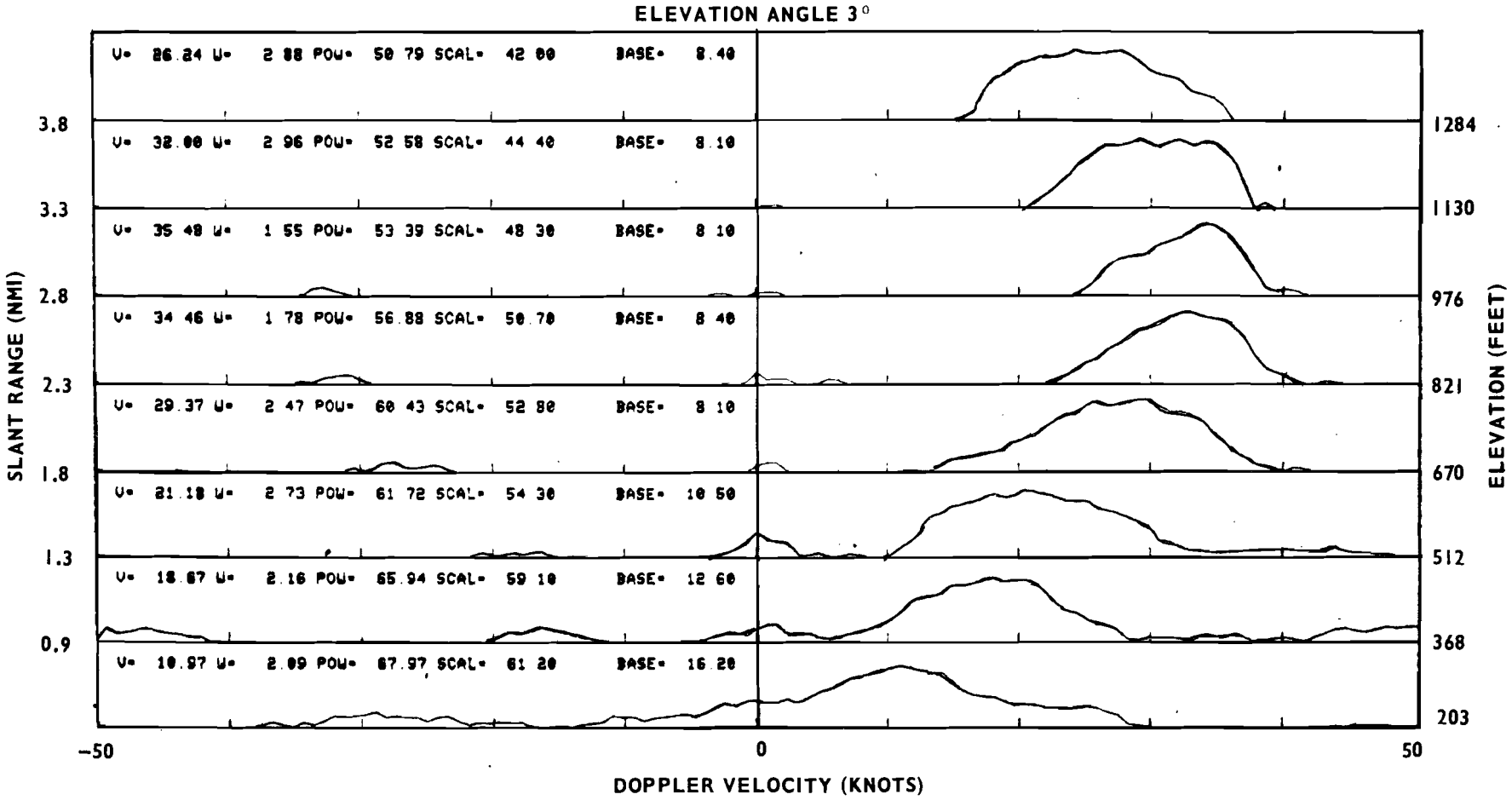

LEGEND:

V=SIGNAL MEAN RADIAL VELOCITY
W=SIGNAL SPECTRUM WIDTH (KNOTS)
POW=SIGNAL POWER (dB)
SCAL= SIGNAL DISPLAY ADJUSTMENT (dB)
BASE=NOISE THRESHOLD (dB)

81-63-9

FIGURE 9. PRECIPITATION SPECTRA

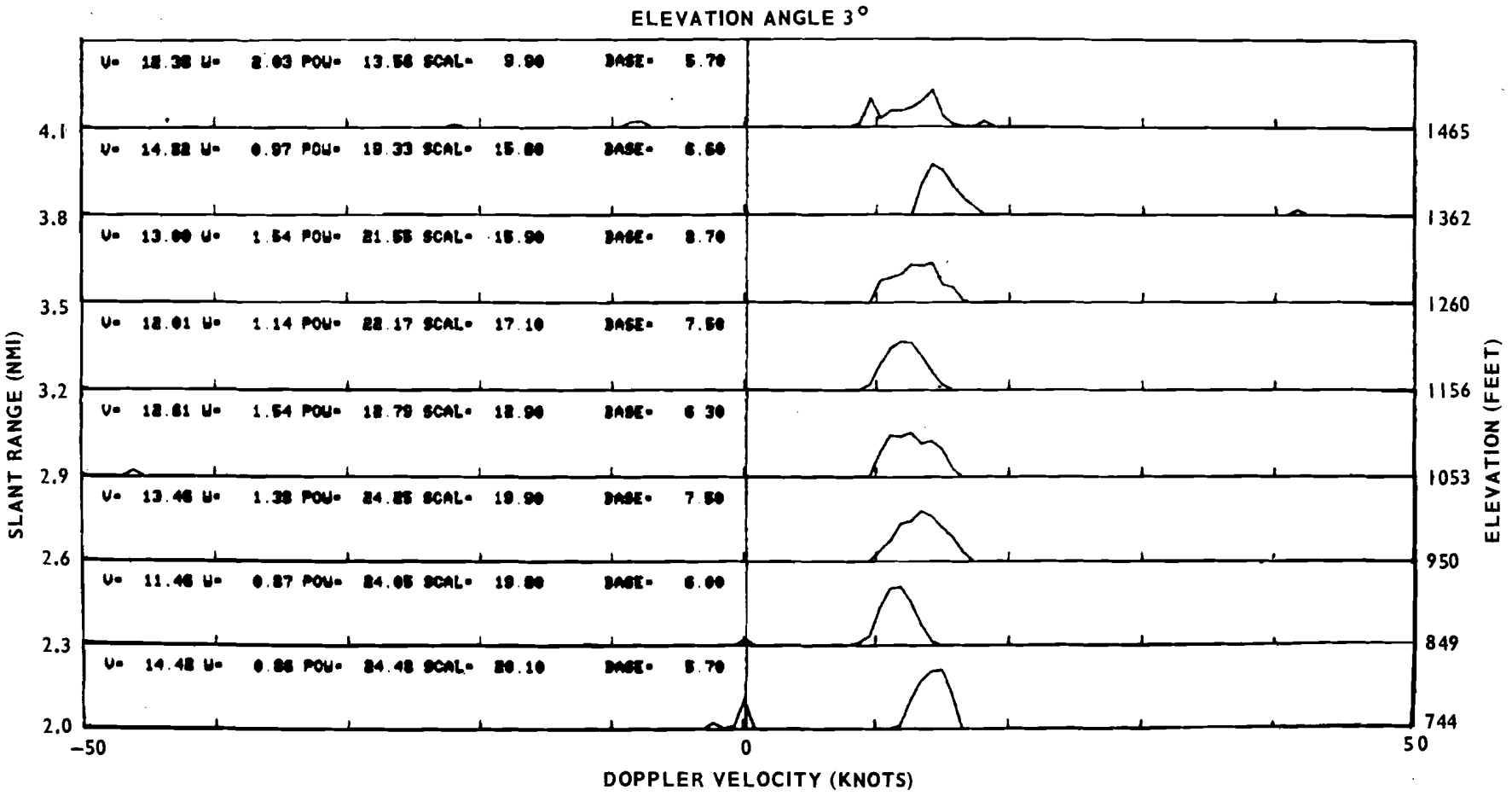

LEGEND:

V = SIGNAL MEAN RADIAL VELOCITY (KNOTS)
W = SIGNAL SPECTRUM WIDTH (KNOTS)
POW = SIGNAL POWER (dB)
SCAL = SIGNAL DISPLAY ADJUSTMENT (dB)
BASE = NOISE THRESHOLD (dB)

81-63-10

FIGURE 10. CLEAR AIR SPECTRA

1. The aircraft flew simulated 3° glide slope approaches directly toward the radar site (assumed to be at the touchdown point) on a heading approximately aligned with the winds. The radar measured the wind components for discrete altitude levels just ahead of the aircraft as it descended.

2. The aircraft flew actual approaches to runway 13-31, while radar data were taken on two azimuths spaced 30° apart covering the runway approach area (as shown in figure 11). Vector winds were computed for discrete altitude levels from wind components on the two azimuths. This two-azimuth pointing technique was discussed by Strauch in reference 4.

The two-azimuth pointing technique provided wind speed from the longitudinal and transverse wind components. Wind directions were determined by appropriate trigonometry. The radar and aircraft headwind/tailwind and crosswind components for the runway azimuth were computed and compared.

It is important to emphasize that the two-azimuth pointing technique is applicable only to horizontally homogeneous winds and, as pointed out in reference 4, should not be used where complex three-dimensional wind fields are expected.

SIMULATED APPROACHES. Radar data were obtained for eight levels from 1,600 to 300 feet above ground level (AGL) (close to mean sea level (m.s.l.) for the Technical Center). The INS aircraft winds corresponding to the altitude levels at which radar data were measured were extracted from the aircraft data printouts. A FORTRAN computer program computed the aircraft headwind/tailwind components and produced statistical summaries comparing radar and aircraft components. The totals for groups of approaches are shown in tables 3 and 4.

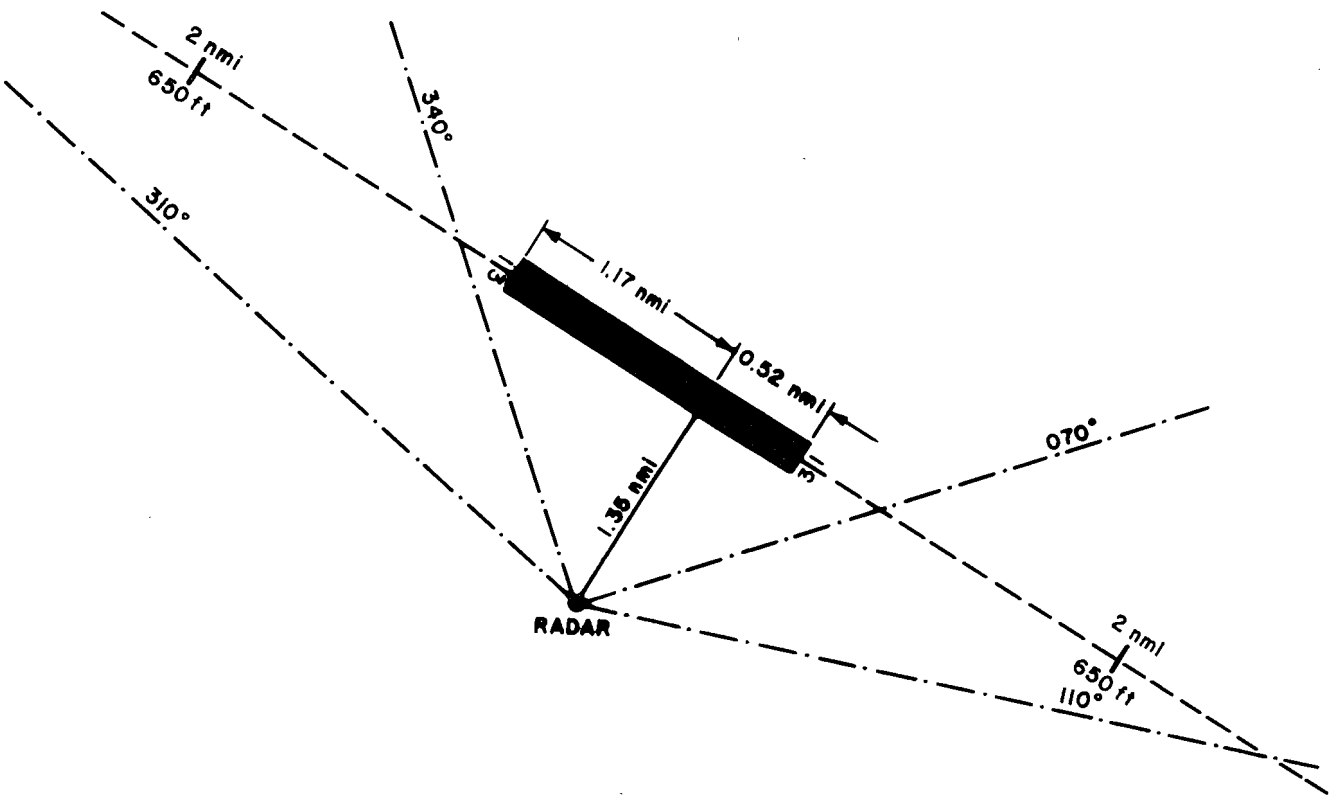

81-63-11

FIGURE 11. RUNWAY 13-31, RADAR LOCATION AND DATA AZIMUTHS FOR WIND DETERMINATION

TABLE 3. COMPARISON OF RADAR AND AIRCRAFT WIND COMPONENTS FOR SIMULATED APPROACHES

Radar*	A/C*	Difference*	Sigma*	Approaches	Total
- 7.8	- 5.6	-2.2	2.9	5	34
-19.5	-18.5	-1.0	2.9	5	35
-14.7	-11.8	-2.9	2.6	5	31

*Values are in knots.
Sigma is standard deviation of differences.

TABLE 4. PRESENTATION OF THE DATA IN TABLE 3 GROUPED BY ALTITUDE

Height (ft)	Radar*	A/C*	Difference*	Sigma*	Distance**	Total
1,600	-14.2	-12.2	-2.0	2.8	4.6	11
1,400	-14.2	-13.1	-1.1	3.0	4.0	14
1,250	-14.9	-12.2	-2.8	3.5	3.5	14
1,050	-14.5	-12.2	-2.3	3.6	2.9	13
900	-14.0	-12.1	-1.9	2.7	2.3	15
700	-14.6	-12.3	-2.3	2.2	1.8	10
500	-13.3	-11.7	-1.6	3.0	1.2	12
300	-12.2	-10.4	-1.8	2.3	0.6	11
ALL	-14.0	-12.1	-1.9	2.9	---	100

*Values are in knots.
**Nautical miles from radar.
Sigma is standard deviation of differences.

Table 3 shows that the radar components averaged 1 to 3 knots larger than the aircraft components, with standard deviations of about 3 knots. The agreement is better than that obtained previously in comparing Doppler-derived aircraft components with the ASR-8 Doppler components (reference 1). The reasons for the constant bias between aircraft and radar-measured winds were apparently due to aircraft problems in both cases. Reference 1 thoroughly discusses the situation regarding the University of Wyoming's Beechcraft. Consultation with the Technical Center's aeronautical engineers revealed that a small error existed in the true airspeed computer in the Center's Gulfstream used in ensuing tests.

A computer program produced the radar winds, the radar and aircraft headwind/tailwind and crosswind components for the glidepath approach azimuths, and the statistical summaries. The totals for two groups of approaches are shown in table 5 (headwind/tailwind comparison) and table 6 (crosswind comparison). The first set of data was for approach 31, the second set was for approach 12. Data are averages in knots for eight altitudes from 1,000 to 200 feet. Sigma is the standard deviation of radar minus aircraft differences.

Table 5 shows that the radar components averaged slightly smaller than the aircraft components, with standard deviations of differences somewhat larger than for the comparisons of table 3.

Table 6 shows that the average crosswind differences are small, but the standard deviations of differences are somewhat larger than with the headwind/tailwind comparisons of table 5.

TABLE 5. COMPARISON OF RADAR AND AIRCRAFT HEADWIND/TAILWIND COMPONENTS FOR ACTUAL APPROACHES

Radar*	A/C*	Difference*	Sigma*	Approaches	Total
18.4	18.8	-0.4	4.7	6	38
21.9	22.9	-1.0	3.2	5	33

*Values in knots, headwind positive.
Sigma is standard deviation of differences.

TABLE 6. COMPARISON OF RADAR AND AIRCRAFT CROSSWIND COMPONENTS FOR ACTUAL APPROACHES

Radar*	A/C*	Difference*	Sigma*	Approaches	Total
-13.6	-13.2	-0.4	7.0	6	38
22.4	21.5	0.9	5.5	5	33

*Values in knots, right crosswind positive.
Sigma is standard deviation of differences.

FAA WJH Technical Center
00090840

RADAR/TOWER WIND COMPARISON. Radar winds determined by using the two-azimuth pointing technique were also compared with winds from a tower-mounted sensor.

The data were processed by a computer program that determined the radar winds and produced the statistical comparisons. Table 7 shows the average winds and the average wind direction/speed differences for discrete groups of observations. This table also shows that the average direction differences and speed differences expand with increasing wind speeds, and that the standard deviations tend to become larger with increasing wind speed.

The radar/tower wind comparison demonstrates the accuracy with which horizontal wind can be determined by the radar.

TABLE 7. RADAR/TOWER AVERAGE WINDS AND DIRECTION/SPEED DIFFERENCES

Radar	Tower	Direction Difference	Direction Sigma	Speed Difference	Speed Sigma	Total
228/12	230/10	-3.0	11.5	1.2	1.8	14
215/14	321/12	-4.6	14.7	2.0	2.7	10
315/19	327/15	-10.3	12.6	4.2	5.3	22
309/25	326/20	-14.8	12.9	5.1	6.9	22

NOTE: Data are averages for discrete groups.
Directions are in degrees.
Speeds are in knots.
Sigmas are the standard deviations of differences.

WEATHER OBSERVATIONS. Data were recorded with various weather conditions showing that radial shear in thunderstorms and squalls can be measured with the system.

SUMMARY OF PHASE 2 RESULTS.

1. In simulated approaches toward the radar site, radar-measured headwind/tailwind components averaged about 2 knots larger than those derived from aircraft winds.

2. In actual approaches to Center runway 13-31, radar-derived headwind/tailwind components averaged about 1 knot less than those derived from aircraft winds in horizontally homogeneous wind conditions. In the crosswinds comparison, radar values averaged about 1 knot more than the aircraft values. For these tests, the radar winds were derived from wind components measured on two azimuths separated by 30°.

3. In a comparison of radar winds measured 200 feet above a tower, with winds from a sensor mounted just above the tower top, the radar wind speeds averaged 1 to 5

knots greater than tower speeds. The speed differences increased with increasing mean wind speed. The radar wind directions averaged 3 to 15 knots less than tower directions, increasing with increased mean wind speed.

4. Radar observations in a thunderstorm and during a sustained squally period showed that potentially dangerous shears could be detected on a continuing basis. However, further investigation is needed to determine operational applications.

5. The application of radar-derived upper winds for weather forecasting as well as ATC was shown by observations taken in storm precipitation.

PHASE 2 CRITICAL CONCLUSIONS.

The radar wind shear system was capable of providing wind velocity and direction information in close agreement with that obtained from an instrumented aircraft and from a meteorological tower in horizontally homogenous wind conditions.

PHASE 3

DISCUSSION.

Phase 3 tests began in the spring of 1980 after installation and checkout of a new antenna feed horn assembly, designed to allow full transmitter power operation without the need for feedhorn pressurization. Data were recorded on a routine basis through the end of the year and also during unusual weather events. Programs were developed and implemented to obtain wind profile measurements using the discrete velocity-azimuth display (VAD) and glide slope scan techniques described in reference 4. The results of these final phase efforts are presented in this section of the report.

Daily Observations. The system was operated as frequently as possible using a wide range of parameter settings while observing and recording data from a variety of meteorological conditions. Previous tests (references 1 and 2 summarized in the first two sections of this report) have shown that the system is vulnerable to a number of performance limitations. The purpose of these observations was to obtain further information on system performance for use in defining any future radar developments in the area of wind shear detection and display.

1. Signal Level Variations. Figures 12 and 13 are examples of data recorded during the two extreme conditions typically encountered in 1980, with most data falling in between. Figure 12 shows the Doppler spectra from a heavy rain shower, with the peak signal power levels approaching 66 dB above the baseline. The undesirable image spectra seen in figure 12 and in two range gates in figure 14 are caused by imbalances in the phase and amplitudes of the I&Q video signals, and by direct current (d.c.) offsets in the analog-to-digital (A/D) converters. If the amplitudes could be balanced to within 10 percent and the phase to better than 5 percent, the image peaks could be kept to more than 25 dB below the main signal (reference 5). However, the very strong weather signals cause limiting in the system whose dynamic range is 54 dB. This and other nonlinearities generate harmonics which further contribute to the image amplitudes.

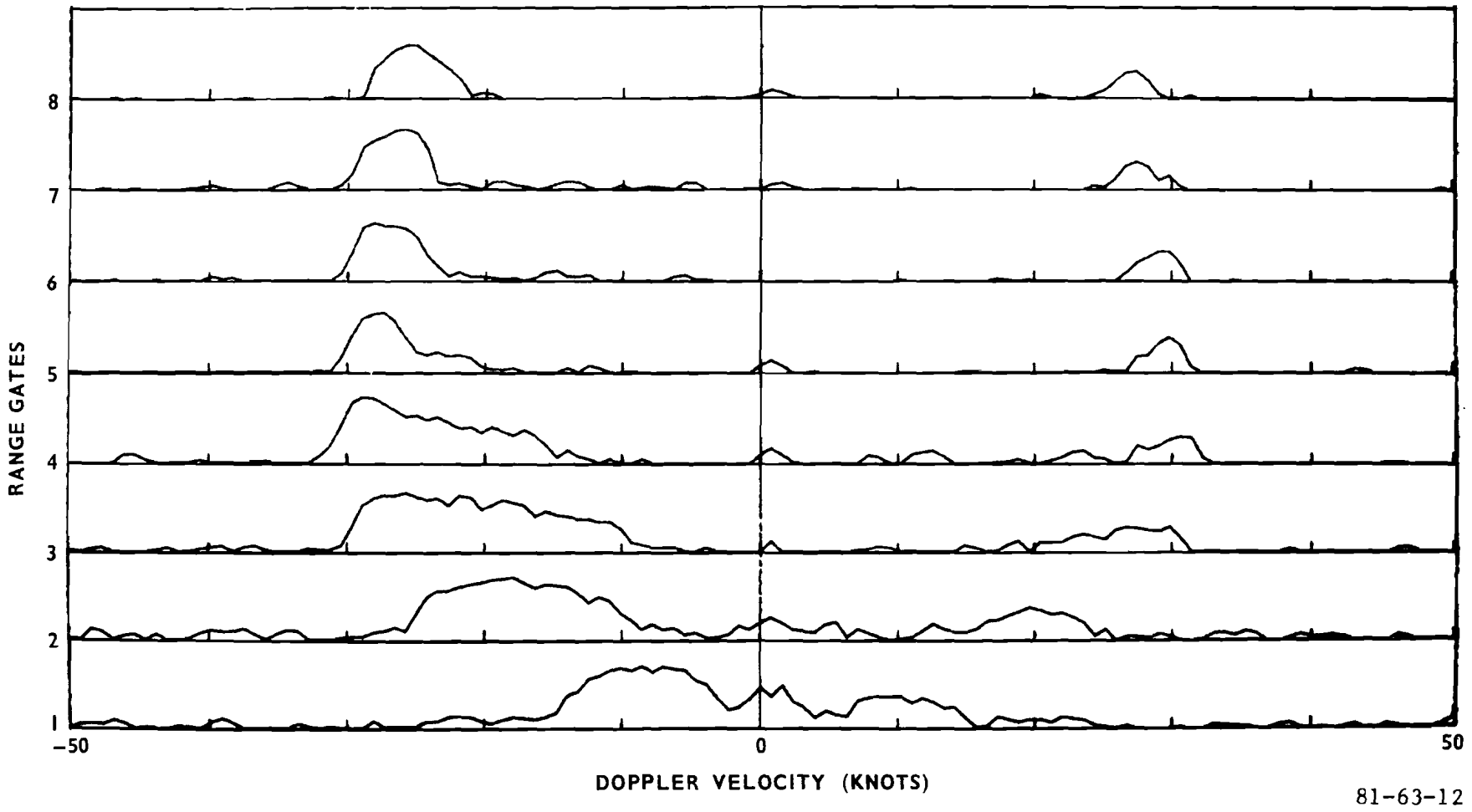

FIGURE 12. DOPPLER SPECTRA OF HEAVY RAIN

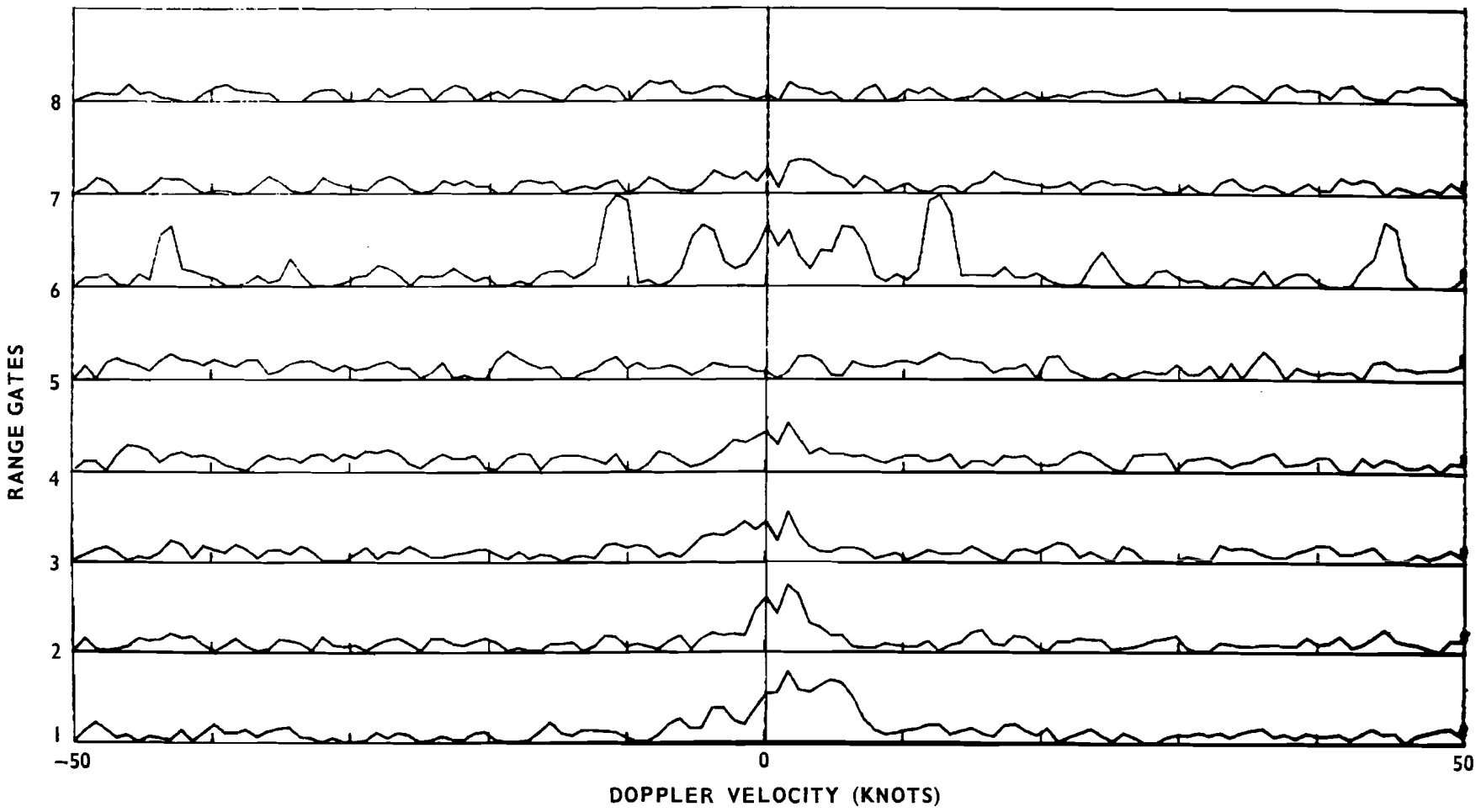

81-63-13

FIGURE 13. CLEAR AIR SPECTRA ON A COLD, DRY DAY

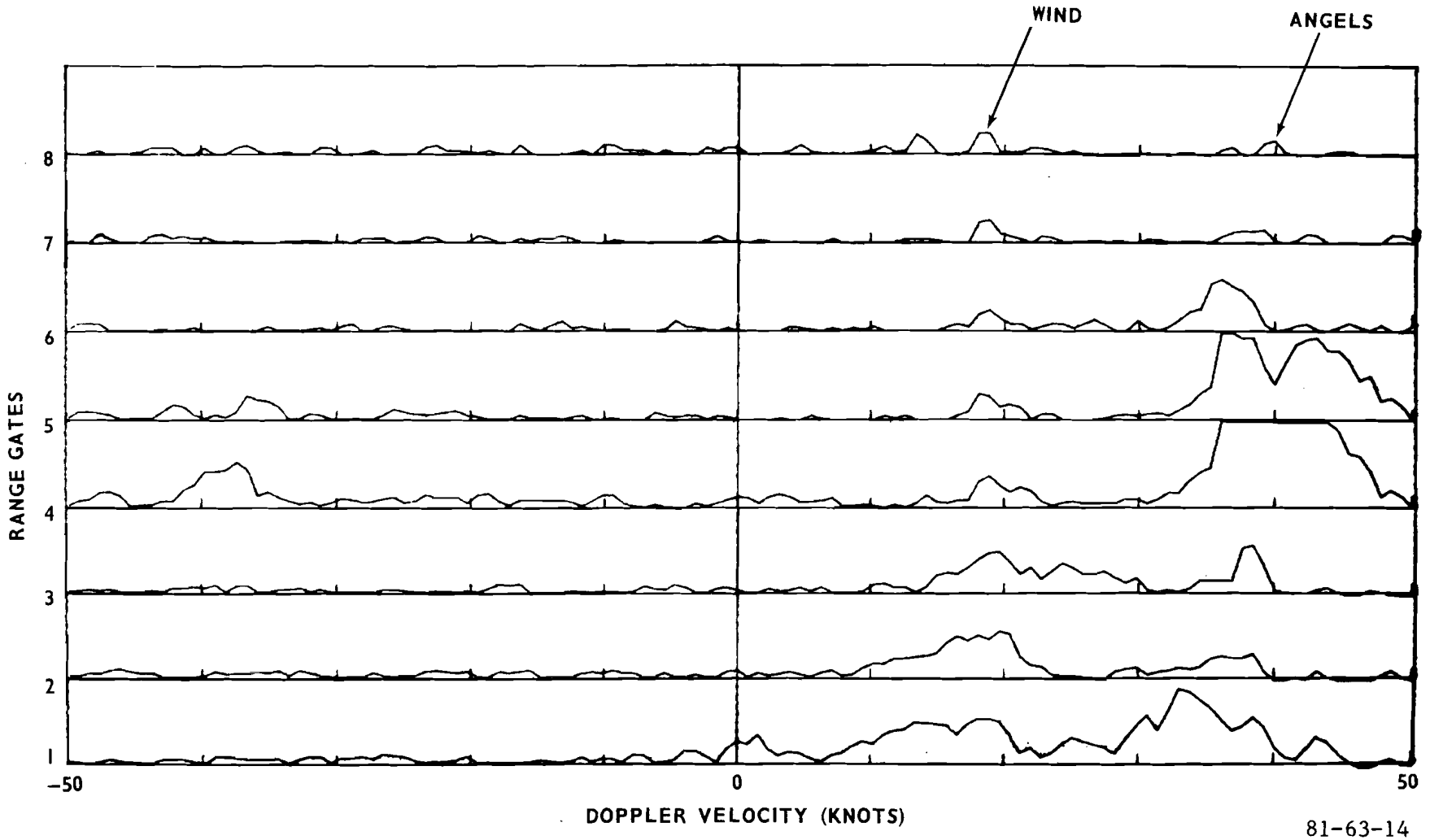

FIGURE 14. SPECTRA OF WIND AND ANOMALOUS SIGNALS

It can be seen that determination of radial velocity in the radar pointing direction presents no problem. Note that system parameters are configured in a fixed glide slope mode, with the antenna at 3° elevation and range sampling occuring at approximately 200-foot intervals along the glide slope from 200 to 1,600 feet altitude. Figure 13 shows the display of returns from optically clear air on a very cold, dry day in December. In this case, note that parameter settings are different with regard to scale, delay, spacing, and antenna position in an attempt to optimize wind measurement; however, the vertical structure being measured is nearly the same except that progression is from 400 to 1,800 feet instead of 200 to 1,600 feet. As can be seen, even with a more sensitive scale setting and increased receiver gain (as evidenced by noisy baseline), wind velocity measurements cannot be determined. The signals in the sixth range gate are a result of receiver saturation from strong side-lobe detected ground clutter.

2. Angel Clutter Effects. Returns from "angels" (ground traffic, birds, and other anomalous moving targets) were detected regularly, and interfered with wind velocity measurements when conditions were unfavorable during periods of clear air observations. It must be emphasized that even with such unfavorable conditions, manual determination of radial wind velocity was still possible, as can be seen in figure 14. In the right side of the display the wind can be seen moving at just less than 20 knots positive, while groups of migrating birds are moving at 35 to 40 knots. The negative Doppler targets in the fourth and fifth range gates are images of the strong positive Doppler signals. In this type of situation the system, as presently configured, would produce erratic and false information if the data were further processed and displayed automatically.

3. Ground Clutter Effects. The Technical Center's ASR-8 is located in a benign ground clutter environment surrounded by flat land, low lying woods, and very few large reflecting structures. Hence, ground clutter, for the most part, had negligible effects on the performance of the Wind Shear Detection System. This was especially so when operating in a fixed glide slope mode, with the antenna at +3° elevation or greater. Examination of various data samples throughout this report shows that only in a few cases, depending on azimuth pointing direction and display gain settings, can limiting effects of ground clutter be seen in one or more range gate samples. With the antenna at elevation angles above 15°, some increase in ground clutter detection was noted because of side-lobe contribution.

However, when operating in the runway-offset glide slope scan mode and with high gain for clear air detection, ground clutter signals prevented detection of winds at the 200- and 400-foot levels. In the glide slope scan (to be discussed later) the position of the radar, with respect to the glide slope runway here at the Center, is such that the antenna must be positioned at very low angles for the lowest altitude levels, resulting in strong clutter returns.

Figure 15 is an example of such data, with receiver saturation causing spectral splatter in the first two range samples, and fixed clutter being displayed in the remaining samples.

THUNDERSTORM GUST FRONT DETECTION. One of the causes of potentially dangerous, low level wind shear is the gust front, or wind outflow in advance of an approaching severe thunderstorm. This has been identified as a prime contributing factor in a number of aircraft accidents. Detection of the phenomena, if possible, has been a major goal of this evaluation.

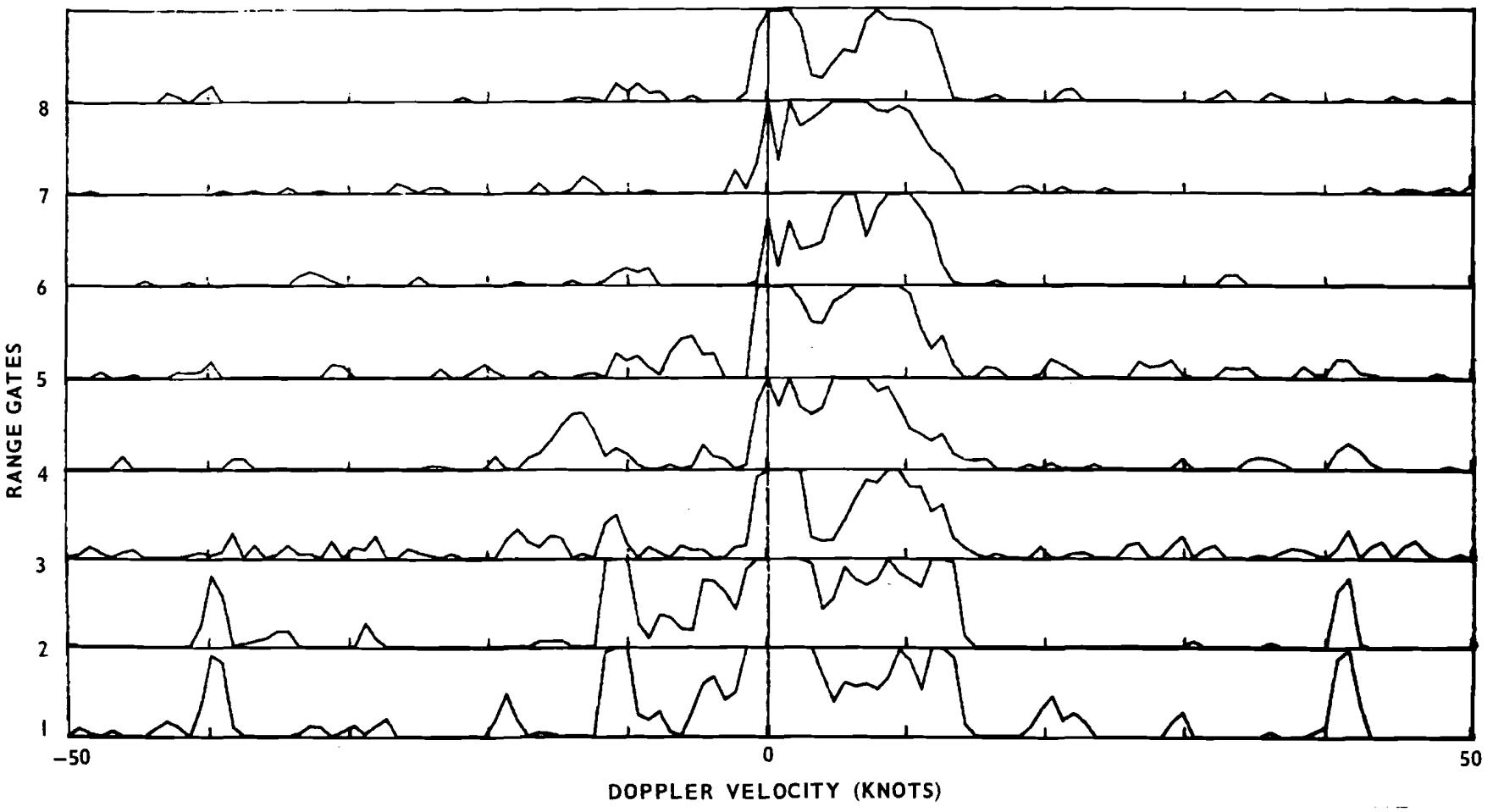

81-63-15

FIGURE 15. GROUND CLUTTER CONTAMINATION AT LOW ELEVATION ANGLES

Under normal conditions the Technical Center area is frequented by very few severe thunderstorms, and seldom are strong winds associated with these storms. This past year was characterized as drier than normal, with even fewer storms. However, on one occasion in April, radar data were obtained as a fast-moving thunderstorm squall line approached from the west. Figure 16 shows profiles of radial wind velocities from two radar observations made just 3 minutes apart. The antenna was at +3° elevation and 270° azimuth, pointing in the direction of the surface wind as determined by the tower-mounted anemometer. At the 300-foot level a distinct bulge, or nose, can be seen in the later profile representing an increase of about 17 knots, going from an earlier reading of 8 knots to a sustained velocity of 25 knots.

On another occasion, 10 days later, data were recorded from a thunderstorm observation. Figure 17 is a radial wind profile from that storm, with the antenna in a +3° fixed glide slope configuration, looking into the direction of the surface wind. In this case the storm appeared to be producing an outflow at a higher altitude level. Note the potentially dangerous wind shear between the 800- and 1,000-foot altitudes, with the radial wind increasing from 26 to 44 knots.

Glide Slope Scan. This is a technique, described in reference 4, for obtaining radial velocity measurements along the glide slope when the radar location is offset from the airport centerfield, as is the case here at the Technical Center. The exact location of the ASR-8, runway orientation, and other particulars are discussed earlier in this report.

A program was developed to obtain data on the approach to runway 13. Radial velocity samplings were made with the antenna at the azimuth and elevation settings shown in table 8. Eight measurements were made at each altitude, starting at the point indicated by the delay in the table, with 1 μs separation between measurements.

The resultant raw data format was similar to the data samples illustrated throughout this report. In order to show the lines of equal Doppler velocities (isodops) in the B-scan presentation suggested in reference 4, the mean of each Doppler spectra was determined manually and plotted.

During the period of time following implementation of this program, no unusual meteorological conditions were present at the Technical Center, hence, an evaluation of this technique's wind shear warning capability was not determined. In every case the wind conditions were so benign and uniform that all the plots of constant radial velocity contours were bunched closely together.

Rather than presenting an actual sample of data, a hypothetical ideal display is shown in figure 18. In this case the data surface is a plane which includes the approach path, radar location, and touchdown point. At each azimuth angle where the radar beam intersects the approach path the radial velocity is displayed as a function of range. Since all points along the range axis correspond to a fixed antenna position, the isodops for uniform winds are horizontal lines. The altitude coordinate is the altitude on the approach path, not the altitude of all data points.

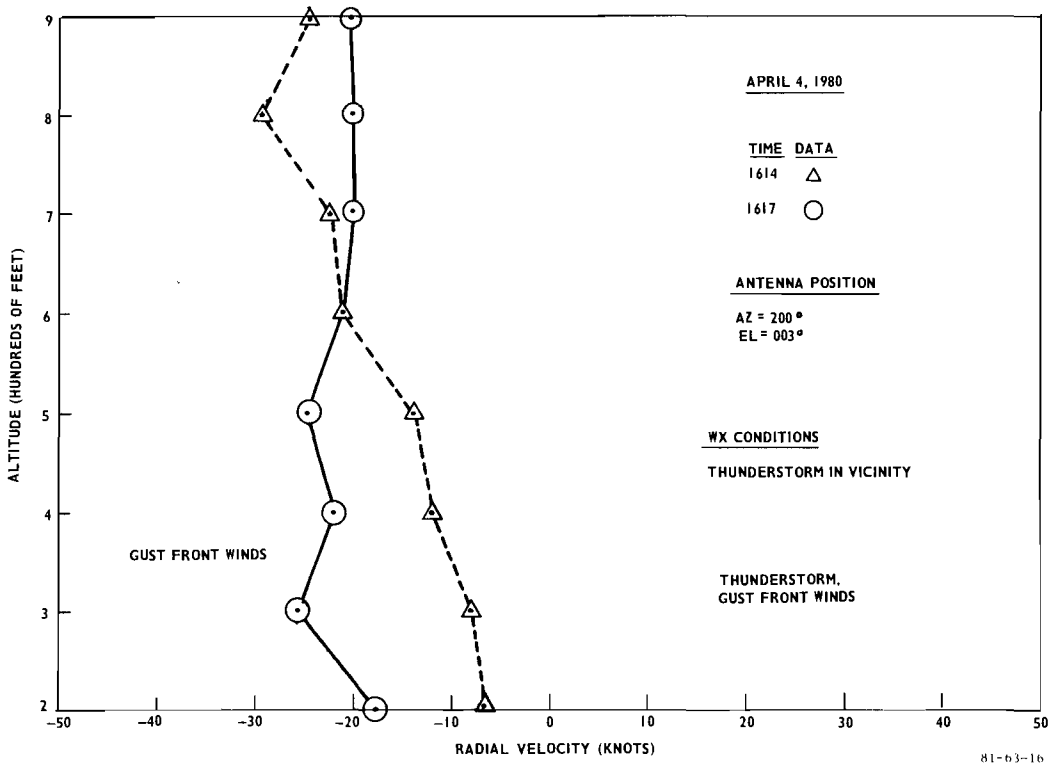

FIGURE 16. THUNDERSTORM GUST FRONT WINDS

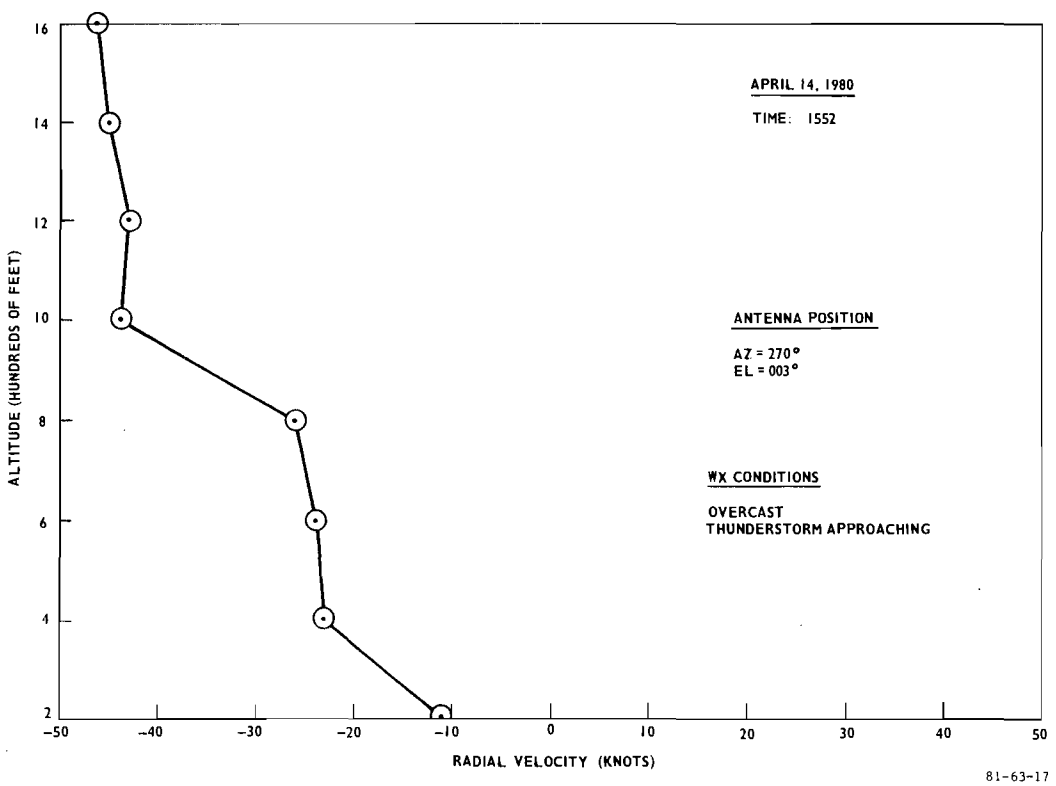

FIGURE 17. THUNDERSTORM WIND OUTFLOW

TABLE 8. SYSTEM PARAMETERS FOR GLIDE SLOPE SCAN

Height*	Azimuth	Elevation	Delay (μs)
1600	311	2.4	76
1400	313	2.3	69
1200	315	2.2	62
1000	317	2.0	54
800	320	1.9	47
600	324	1.7	39
400	330	1.3	33
200	340	0.7	27

Approach runway 13, 3° glide slope

*Along glide slope

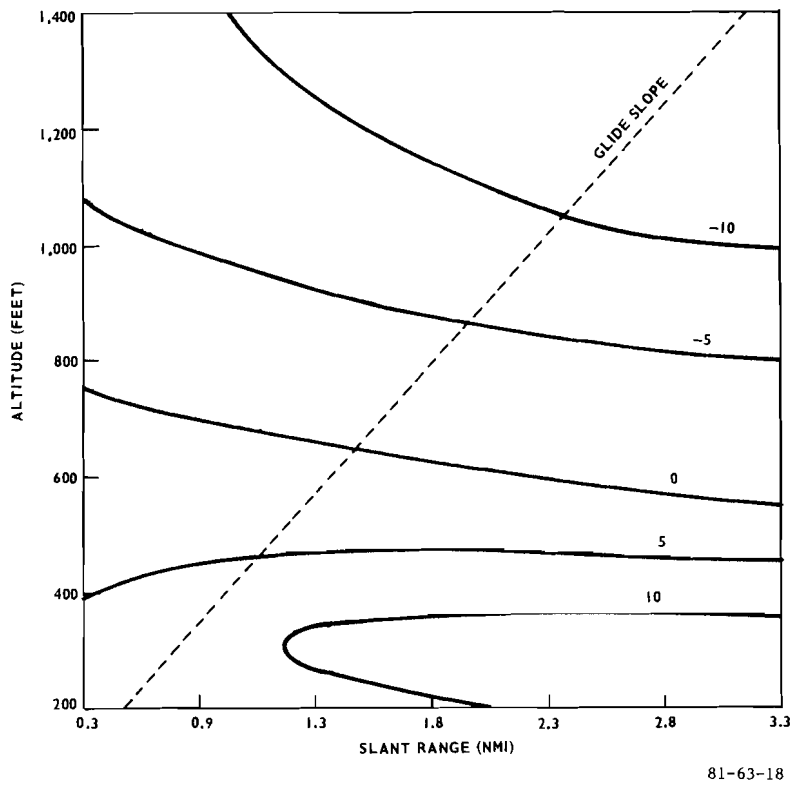

FIGURE 18. CONTOURS OF CONSTANT RADIAL VELOCITY FOR A TYPICAL GLIDE SLOPE SCAN

One of the major problems encountered with this mode of operation was the excessive ground clutter returns at the very low antenna elevation angles as discussed earlier in this report. A sample of the clutter is shown in figure 15. Reference 4 points out that the radial velocity patterns with this type of display are complex and difficult to interpret. The low elevation angles also result in poor vertical resolution.

MODIFIED VELOCITY-AZIMUTH DISPLAY. Reference 4 discusses another technique for measuring wind profiles with Doppler radar known as the VAD method. A simplified version used during these tests, involving measurements of the radial velocity profile at 4 points in azimuth separated by 90°, is also described. The purpose of this method is to allow the use of fixed antennas which are less costly than the single antenna and pedestal required for the continuous scan VAD.

Simplified VAD observations were made on two consecutive days (September 30 and October 1, 1980) while an instrumented aircraft flew approaches to runway 13. Three approaches were made on each day with light northeast to east wind prevailing. The radar antenna elevation angle was 6° and winds were obtained at 200-foot intervals from 200 to 1,600 feet. Radar data acquisition time was 12 minutes centered approximately around the aircraft's two-minute glide slope approach time. Since wind conditions on the two days were similar and data samples small for individual altitudes, the data were summarized in one group. Results for the 38 usable (out of a possible 48) comparisons are shown in table 9.

Table 9 shows reasonable agreement between the two sets of measurements considering the difference in acquisition time and the fact that the radar is offset from the runway 13 approach area approximately 2 to 5 nautical miles. Wind components on some azimuths were, thus, obtained from locations considerably more distant.

TABLE 9. RADAR/AIRCRAFT WIND COMPARISON FOR SIMPLIFIED VAD

Radar	Aircraft	Direction Difference	Direction Sigma	Speed Difference	Speed Sigma	Total
45/15	58/14	-13.4	19.3	0.4	3.4	38

Note: Directions are in degrees. Speeds are in knots. Sigmas are the standard deviations of differences.

SUMMARY OF PHASE 3 RESULTS.

1. During the period of this evaluation the peak signal power levels of the processed Doppler spectra varied over a range from receiver baseline for clear air returns to 66 dB for heavy rain.

2. Receiver dynamic range limitations resulted in undesirable image spectra when strong radar returns are processed.

3. Anomalous moving target signals interfered with routine wind measurements under certain meteorological conditions.

4. Ground clutter had negligible effect on system performance except when the antenna was at elevation angles below 3°, or at high elevation angles where sidelobes create ground clutter returns.

5. Thunderstorm gust fronts and wind outflows were detected on two occasions during these tests.

6. A glide slope scan program was developed and tested. Low level ground clutter returns, poor resolution, and lack of unusual winds prevented complete evaluation of the technique.

7. The modified velocity azimuth display, or 4-point scan, resulted in wind measurements which compared favorably to simultaneously recorded aircraft winds. Radar wind directions averaged 13° less than aircraft and velocities were approximately the same.

PHASE 3 CRITICAL CONCLUSIONS.

The glide slope scan technique did not provide satisfactory operation. The modified velocity azimuth display technique provided satisfactory wind measurements in the horizontally homogenous wind conditions encountered. Clutter signal returns and low amplitude clear air returns in cold, dry conditions limited system performance. Thunderstorm related wind conditions were detected and measured.

OVERALL SUMMARY OF RESULTS

1. Installation and integration of the system with the Technical Center's terminal radar test bed was accomplished without difficulty.

2. Operational parameters and system characteristics were determined and established.

3. Returns from optically clear air as well as from precipitation were obtainable at all times when data were taken.

4. Velocity calibration of the display was completed.

5. Flight tests showed generally good agreement between simultaneously recorded radar and aircraft wind data.

6. In simulated approaches toward the radar site, radar-measured headwind/tailwind components averaged about 2 knots larger than those derived from aircraft winds.

7. In actual approaches to the Center's runway 13-31, radar-derived headwind/tailwind components averaged about 1 knot less than those derived from aircraft in horizontally homogeneous wind conditions. In the crosswinds comparison, radar values averaged about 1 knot more than the aircraft values. For these tests the radar winds were derived from wind components measured on two azimuths separated by 30°.

8. In a comparison of radar winds measured 200 feet above a tower, with winds from a sensor mounted just above the tower top, the radar wind speeds averaged 1 to 5 knots greater than tower speeds. The speed differences increased with increasing mean wind speed. The radar wind directions averaged 3° to 15° less than tower directions, increasing with increased mean wind speed.

9. Radar observations in a thunderstorm and during a sustained squally period showed that potentially dangerous shears could be detected. However, further investigation is needed to determine operational applications.

10. The application of radar-derived upper winds for weather forecasting as well as ATC was shown by observations taken in storm precipitation.

11. During the period of this evaluation, the peak signal power levels of the processed Doppler spectra varied over a range from receiver baseline for clear air returns to 66 dB for heavy rain.

12. Anomalous moving target signals interfered with routine wind measurements under certain meteorological conditions.

13. Receiver dynamic range limitations resulted in undesirable image spectra when strong radar returns were processed.

14. Ground clutter had negligible effect on system performance except when the antenna was at elevation angles below 3°, or at high elevation angles where sidelobes create ground clutter returns.

15. Thunderstorm gust fronts and wind outflows were detected on two occasions during these tests.

16. A glide slope scan program was developed and tested. Low level ground clutter returns, poor resolution, and lack of unusual winds prevented complete evaluation of the technique.

17. The modified velocity azimuth display, or 4-point scan, resulted in wind measurements which compared favorably to simultaneously recorded aircraft winds. Radar wind directions averaged 13° less than aircraft and velocities were approximately the same.

CONCLUSIONS

Based on the results of this investigation, it is concluded that:

1. The Wave Propagation Laboratory (WPL) wind shear system operated satisfactorily with the Federal Aviation Administration (FAA) Technical Center terminal radar test bed. The processing and spectral display of radar returns were shown to be feasible.

2. The system is capable of measuring radial wind components along the simulated flightpath (radial to the radar) flown by the aircraft, thus, a radar located near a runway can measure headwinds or tailwinds along the path of landing or departing aircraft.

3. With the radar offset from the runway and the horizontally homogeneous wind regimes encountered at the Center to date, the two-azimuth pointing method was capable of determining wind components measured by actual runway-oriented flight to within a 1-sigma accuracy of 3 to 7 knots.

4. A comparison of radar and tower winds showed agreement to within a 1-sigma directional accuracy of 11.5° to 14.7°, and a 1-sigma speed accuracy of 1.8 to 6.9 knots for the weather regimes encountered when the radar used a two-azimuth pointing technique.

5. Potentially dangerous radial wind shears associated with the weather encountered during these test were detectable, but further investigation is required to determine operational applications.

6. System limitations in the areas of processing receiver dynamic range and data display can be resolvable through redesign.

7. The glide slope scan was not capable of measuring winds along the glide slope with the radar offset from the runway and the wind regimes encountered.

8. The modified velocity azimuth display is a viable method for determining existence of and measuring horizontally homogeneous airport terminal winds with a single Doppler radar.

RECOMMENDATIONS

It is recommended that:

1. The terminal weather radar test bed system be upgraded through improvements in processing speed, receiver chain dynamic range, and data display to serve as a real-time test bed for future meteorological work.

2. A follow-on effort be established to optimize scanning strategies for hazard detection in nonhomogeneous wind conditions.

REFERENCES

1. Offi, D. L. and Lewis, W., Preliminary Tests of the ASR-8 Wind Shear Detection System, FAA Technical Center, Letter Report, NA-78-59-LR, December 1978.

2. Offi, D. L., Lewis, W., Lee, T., and DeLaMarche, A., Test and Evaluation of the Airport Surveillance Radar (ASR-8) Wind Shear Detection System (Phase II), FAA Technical Center, Interim Report, FAA-RD-80-21A (FAA-CT-80-17A), August 1980.

3. Strauch, R. G., Monthly Progress Letter No. 26, Interagency Agreement, Department of Transportation, WPL, ERL, NOAA, Boulder, Colorado, DOT-FA76WAI-622 Task VII, June 1979.

4. Strauch, R. G. and Sweezy, W. B., Wind Shear Detection with Pulse Doppler Radar, FAA/SRDS, Washington, D.C., Final Report, FAA-RD-80-26, January 1980.

5. Doviak, R. J., Zrnic', D. S., and Sirmans, D. S., Doppler Weather Radar, Proceedings, IEEE, Vol. 67, No.11, pp. 1522-1553.

APPENDIX

University of Wyoming
Department of Atmospheric Science

BEECHCRAFT QUEEN AIR RESEARCH AIRCRAFT MODEL 65-B80

The aircraft is equipped with a variety of sensors, some permanently installed and others installed for specific investigations. A list of measured parameters is given in table A-1. The horizontal wind parameter (item 20 in the table) was of primary importance to these tests. The wind is calculated from the aircraft's true airspeed, true heading, and drift angle determined from onboard Doppler radar processing. Winds are computed at 1-second intervals and stored on magnetic tape for subsequent analysis. The aircraft is also equipped with a computer-directed system for acquisition, recording, and display. The system receives all controls from a minicomputer and may be operated in one of three separate modes: the airborne data acquisition mode, the self-check mode (which is used as a preflight or postflight tool), and the data processing mode. The modes are selected by entering a new program into the memory of the computer.

In the data acquisition mode, the sensor outputs are transferred to the computer through the multiplexer after being signal conditioned. Housekeeping data such as time of day, date, and event information are also multiplexed into the computer. Event information, which is a discrete signal used to indicate selected events such as cloud base, photos, etc., can be received from the pilot position, copilot position, and technician or operator position. Data which are inputted to the computer are formatted and recorded on computer-compatible magnetic tape. The computer also uses very high frequency (VHF) omnidirectional radio range (VOR) and distance measuring equipment (DME) data to compute aircraft position which is recorded on magnetic tape. Selected fault detection and identification during the data collection mission is also provided by the onboard computer. The computer also monitors the status of the tape recorder and performs a "read-after-write" check.

The second mode of operation, which is the self-check mode, switches the system signal-conditioned inputs from the sensor output to the sensor simulator output. The computer controls the simulator and checks the data channel for the desired results. Any deviations from the desired output, within specified tolerances, are indicated and identified on the operator's control panel.

The third mode of operation is the data processing mode, which can only be performed on the ground due to the size of the peripheral equipment required. Raw data are read from the magnetic tape in 1-second blocks, processed, and the computed parameter tabulated using a high-speed line printer located external to the aircraft.

TABLE A-1

The following parameters are computed and are selectable for real-time display at both the cockpit and the cabin display panels.

1. Indicated airspeed (knots)
2. Pressure altitude (inches of mercury (Hg) or millibars)
3. Altitude (feet)
4. Static temperature (for Rosemount and reverse flow probes)
5. Potential temperature (for Rosemount and reverse flow probes)
6. Dew point
7. Depression
8. Specific humidity
9. Equivalent potential temperature (for Rosemount and reverse flow probes)
10. True airspeed (knots)
11. Manifold pressure (inches of Hg)
12. Turbulence (ITU)
13. Liquid water (gm/m^3)
14. DME (nautical miles)
15. VOR (degrees)
16. Heading (degrees)
17. Condensation nuclei concentration ($particles/cm^3$)
18. Rate of climb (feet/minute)
19. Filter sequencer differential flow pressure (inches Hg)
20. Horizontal wind (magnitude - knots; direction - degrees)
21. Virtual potential temperature
22. Vertical wind, meters per second (m/s)

System Recording Capabilities:

Sensor outputs	36 positions
Pilot events	10 positions
Copilot events	10 positions
Technician events	10 positions

System Control Capabilities:

Fault detection system
Calibration system
Cockpit display
Course plotting